Kisoo Yoo[1]
Jaesool Shim[2]
Jin Liu[1]
Prashanta Dutta[1]

[1]School of Mechanical and Materials Engineering, Washington State University, Pullman, WA, USA
[2]School of Mechanical Engineering, Yeungnam University, Gyeongsan, South Korea

Received July 5, 2013
Revised October 1, 2013
Accepted October 16, 2013

Research Article

Efficient algorithm for simulation of isoelectric focusing

IEF simulation is an effective tool to investigate the transport phenomena and separation performance as well as to design IEF microchip. However, multidimensional IEF simulations are computationally intensive as one has to solve a large number of mass conservation equations for ampholytes to simulate a realistic case. In this study, a parallel scheme for a 2D IEF simulation is developed to reduce the computational time. The calculation time for each equation is analyzed to identify which procedure is suitable for parallelization. As expected, simultaneous solution of mass conservation equations of ampholytes is identified as the computational hot spot, and the computational time can be significantly reduced by parallelizing the solution procedure for that. Moreover, to optimize the computing time, electric potential behavior during transient state is investigated. It is found that for a straight channel the transient variation of electric potential along the channel is negligible in a narrow pH range (5∼8) IEF. Thus the charge conservation equation is solved for the first time step only, and the electric potential obtain from that is used for subsequent calculations. IEF simulations are carried out using this algorithm for separation of cardiac troponin I from serum albumin in a pH range of 5–8 using 192 biprotic ampholytes. Significant reduction in simulation time is achieved using the parallel algorithm. We also study the effect of number of ampholytes to form the pH gradient and its effect in the focusing and separation behavior of cardiac troponin I and albumin. Our results show that, at the completion of separation phase, the pH profile is stepwise for lower number of ampholytes, but becomes smooth as the number of ampholytes increases. Numerical results also show that higher protein concentration can be obtained using higher number of ampholytes.

Keywords:
Ampholyte / Isoelectric focusing / Parallel computing / Protein / Segregated method
DOI 10.1002/elps.201300310

Additional supporting information may be found in the online version of this article at the publisher's web-site

1 Introduction

IEF is a useful tool to separate and concentrate amphoteric compounds, such as proteins and peptides by using an external electric field in the presence of a pH gradient [1]. In recent years, IEF has been tested in microdevices [2, 3] because it reduces consumption of samples as well as reagents significantly, allows faster separation with very high resolution [4], and minimizes the sample degradation due to Joule heating [5]. Numerical modeling and simulation of IEF can be an efficient tool to design the microchip for separation and concentration of proteins.

One of the key challenges of IEF simulation is the computational cost as one has to solve a large number of mass conservation equations. In a typical IEF, the pH gradient is formed by 100∼1000 ampholytic components [4]. Thus, depending on the system of interest, one has to solve 100∼1000 mass conservation equations simultaneously. Moreover, in a broad range IEF ($3 < pH < 10$) the concentration difference between ampholytes and hydrogen ion is six orders of

Correspondence: Dr. Prashanta Dutta, School of Mechanical and Materials Engineering, Washington State University, Pullman, WA 99163, USA
E-mail: dutta@mail.wsu.edu
Fax: +1-509-335-4662

Abbreviations: cTnI, cardiac troponin I; **OpenMP**, open multiprocessing

Colour Online: See the article online to view Figs. 2 and 4–6 in colour.

magnitude, which makes the convergence of the numerical solution extremely difficult unless a very small time step or relaxation factor is used. For an unsteady IEF, the required small time step multiplexes the computational expense drastically. Even in a 2D geometry, it may take months to simulate a realistic case with 100 ampholytes in a serial code. Thus, there is a critical need to develop a parallel computational algorithm so that IEF simulation can be completed in reasonable amount of time.

Parallel computing is used in many research fields including meteorology, fluid dynamics, quantum mechanics, etc. to reduce the computational time. Depending on the type of problems, parallel computing methods can be developed based on the coupled or segregated algorithm [6]. The coupled algorithm is generally used for very large number of grid points such as in the computer modeling of the earth atmosphere due to the very large computational domain and long time, or direct numerical simulation of turbulent flow over aircraft due to the very small time and length scales. In the coupled algorithm, the computational domain is decomposed among CPUs and discretized equations are solved concurrently using an efficient direct solver such as Pardiso, Fishpack, etc. [7]. The boundary data treatment is a major issue in the domain decomposition technique used in coupled method. Data sharing can increase the processing time as the number of CPU is increased, which may significantly reduce the parallelization efficiency. On the other hand, in the segregated algorithm individual matrix is formed, for each governing equation for the whole computational domain, and then each matrix is solved independently. The segregated algorithm is generally preferred for problems involving a large number of governing equations, such as Monte Carlo simulations for quantum physics. Although this method uses an iterative procedure until a global convergence is obtained, parallelization can be applied at the computational hot spot without special treatment for the boundary data sharing. In IEF, a large number of mass conservation equations for ampholytes have to be solved to form the required pH profile. Thus, in this study we adopt the segregated algorithm to simulate IEF and the parallelization is only implemented for solving the ampholyte mass conservation equations. We only focus on the separation phase since most of the microchip IEF is used for quick separation before transferring the separands to another column/channel for further processing.

The rest of the paper is organized as follows. In Section 2.1, we briefly review mathematical model developed for 2D IEF [8] along with the method for calculating net charge for proteins from protein sequence described in [9]. The numerical scheme and parallelization technique used in this study are provided in Section 2.2. Then we present IEF simulations to show the transient focusing behaviors of cardiac troponin I (cTnI) and albumin for varying number of ampholytes. We also discuss the effectiveness of parallelization scheme in Section 3. Finally, we present our conclusions in Section 4.

2 Materials and methods

2.1 Theory

2.1.1 Mathematical model of IEF

The mathematical model for IEF has been well developed [10], and it has been used to study 1D [11, 12] and 2D [8] IEF. In this study, we briefly introduce the main governing equations for self-sufficiency and clarity. IEF can be modeled by the mass conservation equation for each ionic component along with the charge conservation and electroneutrality equations. The mass conservation equation for each amphoteric molecule such as proteins and ampholytes can be derived from the individual mass conservation equations of corresponding species as [8]:

$$\frac{\partial}{\partial t}C_i - D_i\nabla^2 C_i - \nabla\cdot(\omega_i\langle z_i\rangle\nabla\phi C_i) = 0 \tag{1}$$

where C_i, D_i, and ω_i are concentration, diffusivity, and electrophoretic mobility of amphoteric component i, $\langle z_i\rangle$ is the net electric charge for the component i that is either calculated from the pK values [13, 14] or found from the titration data [15], and ϕ is the electric potential. In addition to the amphoteric molecules, an IEF system contains other ionic components such as hydrogen (H) and hydroxyl (OH) ions. Mass conservation equations can be derived for both hydrogen and hydroxyl ions using governing Eq. (1). However, in this study, the concentration of hydrogen ions (C_{H}) is calculated utilizing the electroneutrality condition as [8]:

$$C_H - \frac{K_w}{C_H} + \sum_{i=1}^{M}(\langle z_i\rangle C_i) = 0, \tag{2}$$

where M is the number of amphoteric components in the system and K_{w} is the equilibrium constant for water. The electric field ($\vec{E} = -\nabla\phi$) in the mass conservation equation is calculated from the following charge conservation equation:

$$\nabla\cdot\left[\sigma\vec{E} - G\right] = 0. \tag{3}$$

The ionic conductivity (σ) and G are given as:

$$\sigma = F\left[\sum_{i=1}^{M}\left(\left\langle z_i^2\right\rangle\omega_i C_i\right) + \omega_H C_H + \omega_{OH}\frac{K_w}{C_H}\right] \tag{4a}$$

$$G = F\left[\sum_{i=1}^{M}(D_i\langle z_i\rangle\nabla C_i) + D_H\nabla C_H - D_{OH}\nabla\left(\frac{K_w}{C_H}\right)\right]. \tag{4b}$$

Here $\left\langle z_i^2\right\rangle$ is the mean square charge and F is the Faraday constant. Since all the required equations are coupled, they need to be solved simultaneously.

2.1.2 Protein net charge from titration data

The net charge of a protein $\langle z_i \rangle$ can be calculated from reaction constants (pKs), but for most proteins the reaction constants are not readily available. In this section, we present a procedure to find net charge $\langle z_i \rangle$ and mean square charge $\langle z_i^2 \rangle$ by following the method described in [9].

If a protein has multiple charge states, the net charge can be found from the species concentration (S_{ij}) and charge (z_{ij}):

$$\langle z_i \rangle = \frac{\sum_{j=0}^{J} z_{ij} S_{ij}}{C_i}, \tag{5}$$

where j is the index for species of a protein i with $j = 0$ being the most positive. The basic "mass-action" relationship between charge-adjacent species of the same protein is:

$$S_{ij} = S_{ij-1} + H^+. \tag{6}$$

If the dissociation reactions are fast, the reaction constants can be defined as:

$$K_{ij} = \frac{C_H S_{ij-1}}{S_{ij}}. \tag{7}$$

Assuming that protein i has $J+1$ charge states and the state shift occurs by losing 1 proton, species charge (z_{ij}) could be represented as:

$$z_{ij} = z_{i0} - j, \tag{8}$$

where z_{i0} is the most positive charge. Substituting Eqs. (7) and (8) into Eq. (5), one can get:

$$\langle z_i \rangle = z_{i0} - \overline{\nu_i}, \tag{9}$$

where:

$$\overline{\nu_i} = \sum_{j=1}^{J} \left[j \left(\frac{K_{i1} K_{i2} \cdots K_{ij}}{(C_H)^j} \right) \right] \Bigg/ \left\{ 1 + \sum_{j=1}^{J} \left(\frac{K_{i1} K_{i2} \cdots K_{ij}}{(C_H)^j} \right) \right\} \tag{10}$$

Similar to the net charge, the mean square charge of a protein can be defined as:

$$\left\langle z_i^2 \right\rangle = \frac{\sum_{j=0}^{J} z_{ij}^2 S_{ij}}{C_i}. \tag{11}$$

Now substituting Eqs. (7) and (8) in Eq. (11), we have:

$$\left\langle z_i^2 \right\rangle = (z_{i0})^2 - 2 (z_{i0} - \overline{\nu_i}) \cdot \overline{\nu_i} + \overline{\nu_i^2}, \tag{12}$$

where:

$$\overline{\nu_i^2} = \sum_{j=1}^{J} \left[j^2 \left(\frac{K_{i1} K_{i2} \cdots K_{ij}}{(C_H)^j} \right) \right] \Bigg/ \left\{ 1 + \sum_{j=1}^{J} \left(\frac{K_{i1} K_{i2} \cdots K_{ij}}{(C_H)^j} \right) \right\} \tag{13}$$

Equations (5)–(13) are also applicable for ampholytes. Equations (12) and (13) can be used to find the mean square charge if the reaction rate constants are known. Alternatively, it can be obtained by manipulating the titration data. From the known titration curve, $\langle z_i \rangle = f_i(pH)$, Eq. (9) can be rewritten as:

$$\overline{\nu_i} = z_{i0} - f_i(pH). \tag{14}$$

Also we can differentiate Eq. (10) with respect to C_H to get:

$$\overline{\nu_i^2} = -(C_H) \frac{d(\overline{\nu_i})}{d(C_H)} + (\overline{\nu_i})^2. \tag{15}$$

Substituting Eq. (14) in Eq. (15), we get:

$$\overline{\nu_i^2} = -\frac{1}{\ln(10)} \frac{df_i(pH)}{dpH} + \left[(z_{i0})^2 - 2 z_{i0} f_i(pH) + [f_i(pH)]^2 \right]. \tag{16}$$

Now from Eqs. (12), (14) and (16), an expression for the mean square charge can be obtained as:

$$\left\langle z_i^2 \right\rangle = [f_i(pH)]^2 - \frac{1}{\ln(10)} \frac{df_i(pH)}{dpH}. \tag{17}$$

2.2 Numerical scheme

2.2.1 Parallelization procedure for IEF

There exist two different methods for executing parallel programs: open multi-processing (OpenMP) and message passing interface (MPI). Selection of appropriate method depends on the architecture of the computer and application type. For memory demanding applications MPI would be more suitable, while for CPU demanding applications OpenMP would work better. In this study, we present a parallelization scheme for a microchip IEF based on the segregated algorithm using OpenMP because of the simplicity to get an efficient implementation in a high performance desktop computer. The basic features of the segregated scheme are shown in Fig. 1. In this scheme, one or more mass conservation equations can be solved by a CPU, and there is no data sharing during the solution process of mass conservation equations. Thus, unlike the coupled method, the computational domain is not shared among CPUs, which eliminates the uncertainties in boundary conditions. Once the concentration for each component is obtained from the mass conservation equations, the charge conservation, and electroneutrality equations are solved serially. If a converged solution is obtained for all variables, the solution process proceeds to the next time step using the current solution as the initial conditions. Otherwise, the iteration process is repeated until a convergence is achieved.

2.2.2 Numerical methods

In this work, the finite volume method was used to simulate IEF in a 2D microchannel. Discretized algebraic equations are obtained using the power law scheme for both the mass

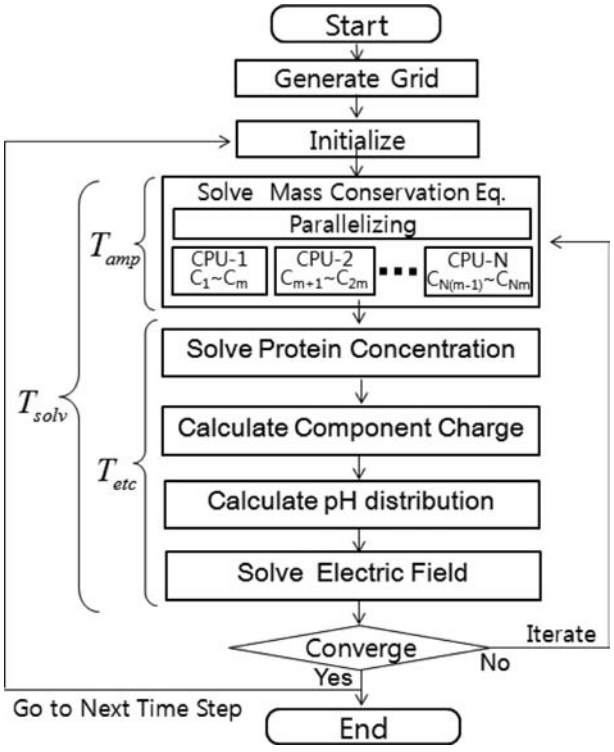

Figure 1. A parallel numerical algorithm for simulation of IEF using the segregated method. Only the solver for the ampholyte mass conservation equations is parallelized in this segregated scheme.

conservation and charge conservation equations. Thomas algorithm is used to solve the tri-diagonal system of linear algebraic equations [16, 17]. As mentioned earlier, the ampholyte mass conservation equations are solved concurrently by applying parallel computing, while the charge conservation equation and protein mass conservation equations are solved sequentially. The tolerances for the mass and charge conservation equations are 10^{-6} and 10^{-4}, respectively. Numerical simulations are performed on an Intel Xeon 2.4 GHz (32 threads).

2.2.3 Parallel computing efficiency

In a serial computation scheme, the time required for all calculations can be defined as:

$$T_{solv,s} = T_{amp} + T_{etc}, \tag{18}$$

where T_{amp} is the CPU time required to solve all ampholyte concentrations serially and T_{etc} is the time required for solving the other equations including the mass conservation equations for proteins as well as the charge conservation equation and electroneutrality equation as shown in Fig. 1. Thus, the fraction of time taken to solve the ampholyte equations can be calculated as:

$$g = \frac{T_{amp}}{T_{solv,s}}. \tag{19}$$

Theoretically, the simulation time of a parallel computation ($T_{\text{solv,p}}$) can be calculated as:

$$T_{solv,p} = \frac{T_{amp}}{N_{CPU}} + T_{etc}, \tag{20}$$

where N_{CPU} is the number of CPUs. Substituting Eqs. (18) and (19) into (20), a relationship between parallel and serial computing time can be obtained as:

$$T_{solv,p} = \frac{g}{N_{CPU}} T_{solv,s} + (1-g)\, T_{solv,s}. \tag{21}$$

Note that Eq. (21) is very similar to Amdalh's law [18]. Thus for the parallel computing, the theoretical speedup value can be obtained as:

$$\frac{T_{solv,s}}{T_{solv,p}} = \frac{1}{g/N_{CPU} + (1-g)}. \tag{22}$$

3 Results and discussion

IEF is simulated in a 2D straight microchannel (length = 1 cm and width = 50 μm). Electric field is applied in the microchannel by applying constant electric potential in the anodic and cathodic side. In this study, the anodic potential is 200 V, while the cathode is ground. For simplicity biprotic ampholytes are chosen, and the isoelectric points (p*I*s) of ampholytes are uniformly spaced within the channel to form a pH profile in the absence of acid and base at the anodic and cathodic column ends. The absolute mobility and ΔpK of each component are 3.0×10^{-8} m^2/V·s and 1.5, respectively. Serum albumin and cTnI are selected as sample proteins. The titration data [15] of these two proteins are obtained from the protein data bank (http://www.uniprot.org), and titration curves are generated using Fourier series for better estimate of the mean square charge and net charge. The resultant titration curves are shown in Supporting Information Fig. 1 for both proteins in Supporting Information. The effect of ionic strength [19, 20] on the effective mobility of proteins and ampholytes is not considered in this study because of their negligible role in IEF [21]. Also the electric field induced EOF and Joule heating effect are not considered in this study.

3.1 Optimization of the algorithm

To optimize the simulation time, we first studied an IEF in the presence of 24 carrier ampholytes in an applied electric field. For simplicity, only cTnI is selected as the sample protein for focusing in a pH range of 6∼8. We particularly selected a narrow range because of its relevance in microchip-based IEF. Cui et al. [4] has shown that the separation resolution can be improved significantly using narrow pH range IEF.

Figure 2A shows the electric potential distribution at different times during the separation phase. As seen from the transient profiles, the electric potential is nearly independent

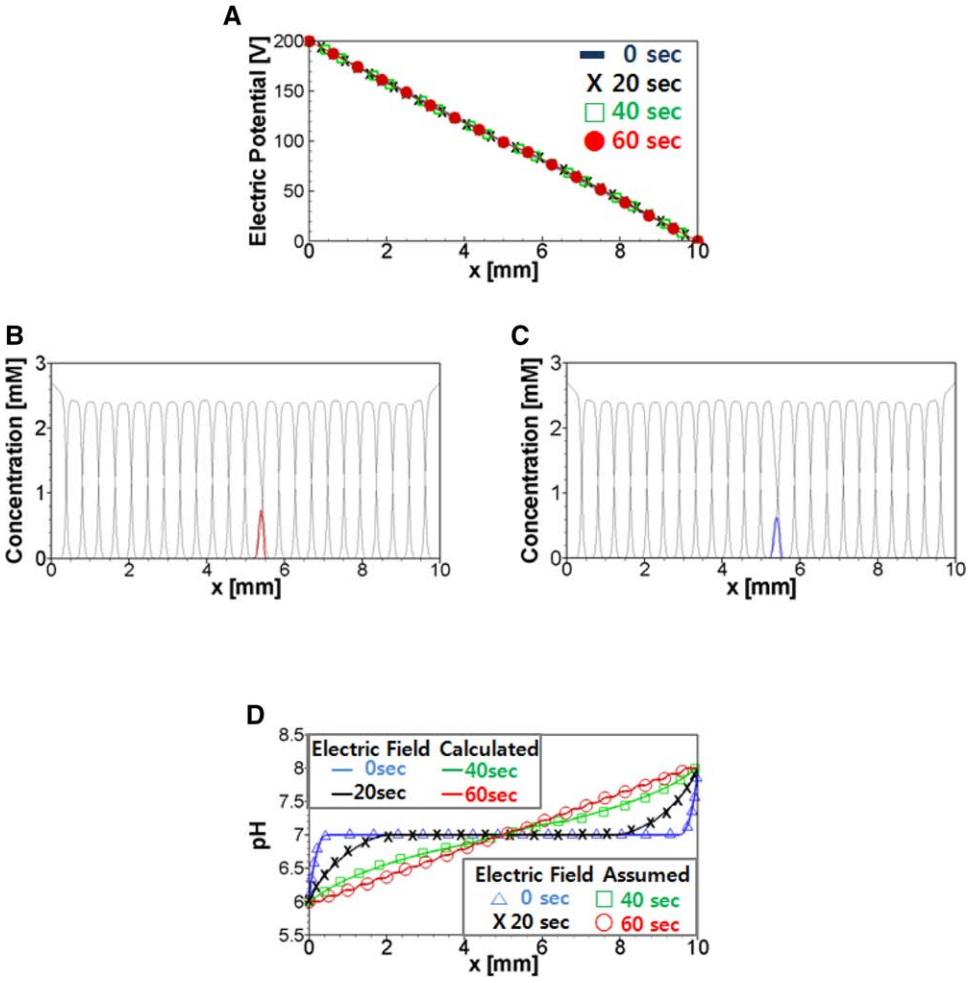

Figure 2. (A) Potential distribution along a straight microchannel at different time of IEF. Twenty-four ampholytes and one protein are used for this simulation. The initial concentration of ampholytes and proteins are 0.1 and 0.01 mM, respectively. Concentration distributions for protein and ampholytes at the end of separation phase for (B) case-A and (C) case-B. (D) The pH distributions during different stages of IEF (Solid lines: IEF simulation results from case-A, Symbols: IEF simulation results from case-B). Very similar results are obtained for both case A and B.

of time. This is due to the fact that in the charge conservation equation, G is almost three order magnitudes smaller than the $\sigma\vec{E}$. These results are in line with the findings of Mosher and Thormann [22, 23] for narrow pH range IEF. Since electric potential does not change appreciably, it is advisable not to solve the charge conservation equation after the first time step to reduce the overall computational time for narrow pH range IEF. To proof our hypothesis, we also simulate IEF without solving the charge conservation equations after the first time step. The concentration profiles are shown in Fig. 2B and C when the electric potential is calculated from the charge conservation equation at every time step (Case A) and only at the first time step (Case B), respectively. In both cases, parallel scheme is used to solve the mass conservation equations for ampholytes. As shown, in both cases the protein is focused at its pI point, while the ampholytes are positioned at their respective locale to form pH profile. The protein is concentrated ~90-fold from its initial uniform concentration of 0.01 mM. Clearly no discernible differences are found between two cases for both ampholytes and proteins.

The time evolution of pH profile is shown in Fig. 2D for both cases. As expected, 24 ampholytes form a step-wise pH profile. The pH profile will be linear once the number of ampholytes is increased to realistic value as presented later. Similar to the concentration and electric potential profiles, there is no noticeable difference between the pH profiles for 24 ampholytes between two cases. The results presented in Fig. 2 suggest that the solution of charge conservation equation is not necessary after the first time step in narrow pH range IEF. It is expected that the elimination of this charge conservation equation will save the computational time significantly as this equation is solved serially in our proposed algorithm. However, one has to solve for charge conservation equation during each time step for broad pH (3~10) range IEF. Our simulation results also show that uniform electric field in a straight microchannel is still a reasonable assumption for the intermediate pH (4~9) range IEF.

Figure 3 shows the time saved by the parallel computing as well as by the elimination of the charge conservation equation for the system. As the number of CPUs is increased from 1 to 4, the time taken for the solution of ampholyte mass conservation equations is decreased significantly. However, the time reduction was not proportional with the number of CPUs. There are two possible explanations for that. First, in parallel computing there is overhead cost related to assignment of job to individual CPUs. Second, 100% load balance

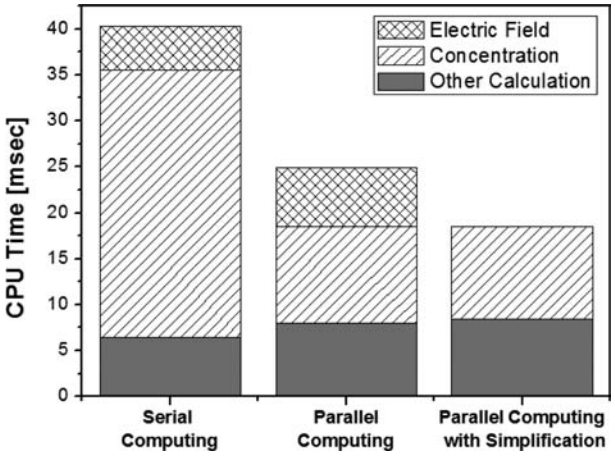

Figure 3. Average CPU time required per time step ($\Delta t = 0.001$ s) to solve different equations in IEF. Results are averaged over 50 000 time steps. All simulation conditions are same as in Fig. 2.

is impossible among CPUs in parallel computing since each mass conservation equation has different level of convergence issue. Nevertheless, for large number of ampholytes, the simulation time can be decreased significantly using parallel algorithm as shown in the next section. Figure 3 also shows that 25% reduction in computation time can be achieved if the charge conservation equation is neglected. The rest of the results are obtained for case B only considering the narrow pH range IEF, in which the charge conservation equation is solved only during the first time step.

3.2 Simulation of a realistic IEF

To form a linear pH profile along the channel, we have selected a larger system consisting of 192 ampholytes in a pH range of 5–8. IEF simulation is performed to separate two proteins: serum albumin and cTnI from an initial mixture of ampholytes. The initial concentration for ampholytes and proteins are 0.1 mM and 0.01 mM, and the initial pH and electric potential are 6.5 and 100 V throughout the channel. Figure 4 shows the IEF results for 192 ampholytes and two proteins. Both concentration profiles and pH distributions are presented for some selected times. At the early stage of focusing, ampholytes closest to the electrode reservoirs start focusing at their respective p*I* points forming a pH slopes only at two ends as shown in Fig. 4A. On the other hand, ampholytes having p*I* points at the middle section of the channel almost remain at the initial condition. As the time progresses, all ampholytes start to focus at their p*I* points and a pH profile is developed throughout the channel. At the completion of separation phase (Fig. 4C), all ampholytes reach almost same concentration along the channel, unless the p*I* point of an ampholyte is very close to the p*I* point of a protein. The numerical results show that, at the completion of separation phase, the concentration of ampholytes has increased 80-folds of its initial value. Similarly, the concentration factor for the cTnI and serum albumin are 110 and 150, respectively. Figure 4C also illustrates that an almost linear pH profile is formed for 192 ampholytes as opposed to stepwise pH profile observed in Fig. 2A in which 24 ampholytes are used for pH gradient formation.

Figure 5 shows the CPU time using 1, 2, 4, 8, and 16 CPUs. The CPU time is significantly reduced when we increase the number of CPU from 1 to 2, but the benefit of

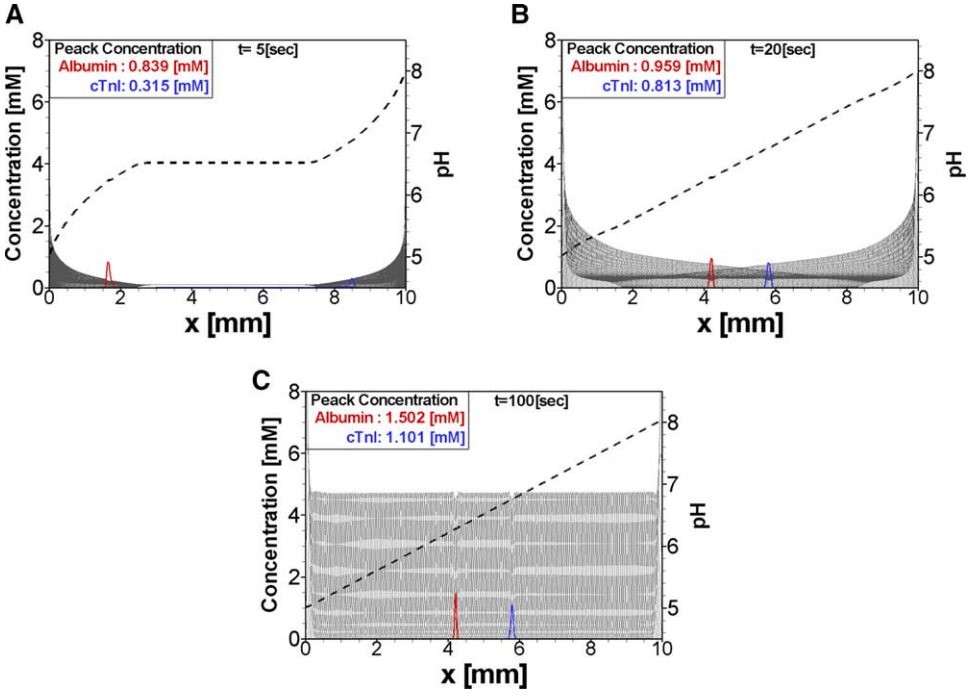

Figure 4. Concentration distributions for proteins and ampholyte along a 2D straight microchannel at (A) $t = 5$ s, (B) $t = 20$ s, and (C) $t = 100$ s. One hundred ninety-two ampholytes and two proteins are used for this simulation. The pH profiles are also shown at each frame with a dash line. The initial concentration of ampholytes and proteins are 0.1 and 0.01 mM, respectively. The anode potential is 200 V, while the cathode is grounded. The spatial grid size is 1 micron and the time step is 1 ms.

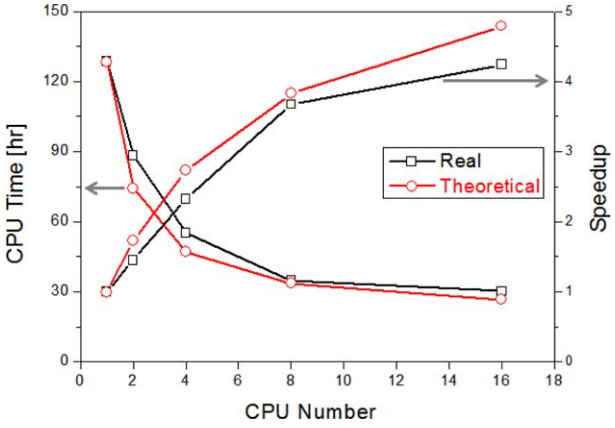

Figure 5. Computational time required to reach 1 s simulation time using different number of CPUs. The second vertical axis shows the speedup of the proposed algorithm. The numerical (real) speedup closely follows the theoretical speedup indicating an efficient algorithm.

parallel algorithm is decreased with further increase. This is due to the fact as the number of CPU increases, the portion of parallelized procedure decreases compare to the whole procedure because the time required for other calculations such as protein concentration, net charge calculations, etc. remains the same. Moreover, excessive memory access problem is partly responsible for the computational slow down if more than eight CPUs are used. A brief discussion on excessive memory access is provided in the Supporting Information.

We also present the theoretical computational time for parallel computing based on Eq. (15). Although both theoretical and real computational times follow the same trend, there are some differences between the two. The real computation time is higher than estimated time because the theoretical computation time is estimated under the assumption that the parallel code is 100% efficient. However, a parallel code cannot work at 100% efficiency because of the load imbalance among the CPUs. Figure 5 also shows speedup for different number of CPUs. The real speedup is lower than the theoretical one because of the reasons explained above.

3.3 Effects of number of ampholytes in protein behavior

We investigate the effect of number of ampholytes in forming pH profile to facilitate the focusing of proteins. Simulations are carried out for different number of ampholytes (48, 96, and 192) to separate cTnI and albumin from an initial uniform mixture as described in the earlier section. For this simulation the spatial grid size is 1 μm and the time step is 1 ms. Figure 6 shows the protein concentrations at different times for different number of ampholytes. As the number of ampholytes increases, the peak concentration of proteins increases for both albumin and cTnI. This is due to the fact the pH gradient is very sharp to form a tightly focused band for higher number of ampholytes (See inset of Fig. 6A). As

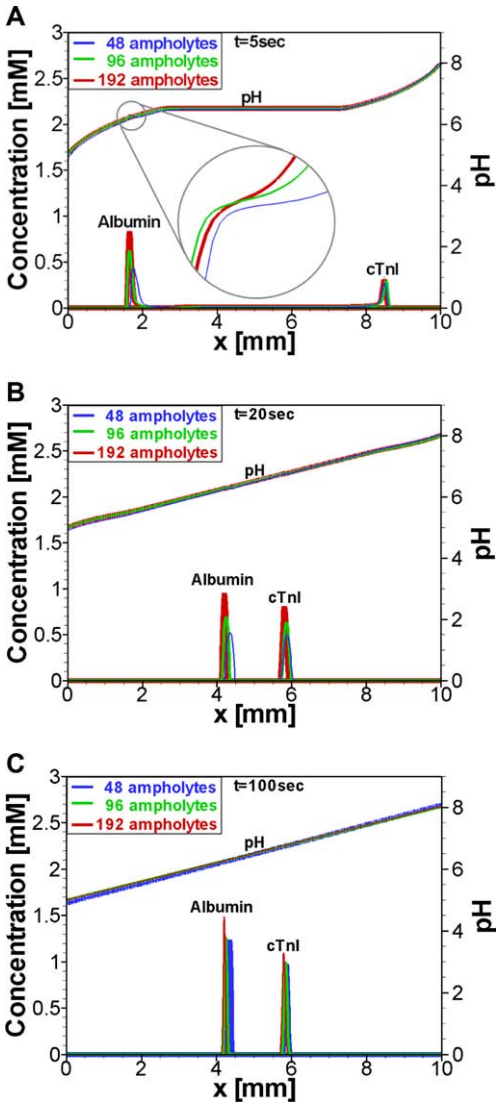

Figure 6. Effect of number of ampholytes in protein focusing trend. All other simulation conditions are same as in Fig. 4.

the number of ampholytes decrease, the pH profile flattens results in a broader peak. These results also show that concentration of albumin is much higher than cTnI. Albumin forms tighter bands compare to cTnI because the slope of the titration curve is much higher for albumin compare to cTnI (see Supporting Information Fig. 1). Based on the titration curve obtained from experiment, the value of (dz/dpH) is –11 and –2.5 for albumin and cTnI, respectively. These results explain that why cTnI cannot be concentrated as much as albumin in microchip IEF and ITP [24, 25].

4 Concluding remarks

A parallel algorithm is developed to simulate IEF in microfluidic devices. The parallelization scheme is based on the segregated algorithm in which the mass conservation

equations are solved in parallel using the OpenMP. The numerical model is further optimized by dropping the solution process for charge conservation equation after first time step as the transient change of potential distribution is negligible in narrow pH range (5∼8) IEF to make any discernible effect in ampholyte and protein behavior. The numerical method is used to simulate IEF for varying number of ampholytes ranging from 24 to 196 to form pH profile in a straight microchannel. Numerical results show that the number of ampholytes has a significant influence on the predicted shape of protein concentration profile. The peak concentrations of proteins are higher for large number of ampholytes. Also, the concentration factor of albumin is much higher than that of cTnI.

The proposed parallelization scheme is very effective in reducing the overall computational time for simulation of large number of ampholytes. The microchip IEF results can be obtained for 192 ampholytes and two proteins in couple of days using the parallel scheme with eight CPUs that will otherwise be prohibitive for a serial code. Ideally, further reduction in the simulation time can be obtained by parallelizing the whole algorithm. However, in reality, it may not be the case because of the data sharing among CPUs. It might further worsen if data sharing takes place among nodes.

This work was supported in part by the US National Science Foundation under Grant No. CBET 1250107 and in part by the Yeungnam University research grants in 2013.

The authors have declared no conflict of interest.

5 References

[1] Righetti, P. G., *Isoelectric Focusing: Theory, Methodology, and Applications*, Elsevier Biomedical Press, Amsterdam 1983.

[2] Herr, A. E., Molho, J. I., Drouvalakis, K. A., Mikkelsen, J. C., Utz, P. J., Santiago, J. G., Kenny, T. W., *Anal. Chem.* 2003, *75*, 1180–1187.

[3] Cui, H. C., Horiuchi, K., Dutta, P., Ivory, C. F., *Anal. Chem.* 2005, *77*, 1303–1309.

[4] Cui, H. C., Horiuchi, K., Dutta, P., Ivory, C. F., *Anal. Chem.* 2005, *77*, 7878–7886.

[5] Rathore, A. S., *J. Chromatogr. A* 2004, *1037*, 431–443.

[6] Hanby, R. F., Silvester, D. J., Chew, J. W., *Int. J. Numer. Methods Fluids* 1996, *22*, 353–373.

[7] Schenk, O., Gaertner, K., *Electron. Trans. Numer. Anal.* 2006, *23*, 158–179.

[8] Shim, J., Dutta, P., Ivory, C. F., *Electrophoresis* 2007, *28*, 572–586.

[9] Mosher, R. A., Dewey, D., Thormann, W., Saville, D. A., Bier, M., *Anal. Chem.* 1989, *61*, 362–366.

[10] Bier, M., Palusinski, O., Mosher, R., Saville, D., *Science* 1983, *219*, 1281–1287.

[11] Mosher, R. A., Breadmore, M. C., Thormann, W., *Electrophoresis* 2011, *32*, 532–541.

[12] Thormann, W., Kilar, F., *Electrophoresis* 2013, *34*, 716–724.

[13] Mosher, R. A., Saville, D. A., Thormann, W., *The Dynamics of Electrophoresis*, VCH, Weinheim 1992.

[14] Shim, J., Dutta, P., Ivory, C. F., *AIChE J.* 2008, *54*, 2238–2249.

[15] Tanford, C., Roxby, R., *Biochemistry* 1972, *11*, 2192–2198.

[16] Shim, J., Dutta, P., Ivory, C. F., *Electrophoresis* 2008, *29*, 1026–1035.

[17] Shim, J., Dutta, P., Ivory, C. F., *J. Nanosci. Nanotechnol.* 2008, *8*, 3719–3728.

[18] Hill, M. D., Marty, M. R., *Computer* 2008, *41*, 33–38.

[19] Vcelakova, K., Zuskova, I., Kenndler, E., Gas, B., *Electrophoresis* 2004, *25*, 309–317.

[20] Zuskova, I., Novotna, A., Vcelakova, K., Gas, B., *J. Chromatogr. B* 2006, *841*, 129–134.

[21] Shim, J., Dutta, P., Ivory, C. F., *Electrophoresis* 2009, *30*, 723–731.

[22] Mosher, R. A., Thormann, W., *Electrophoresis* 2008, *29*, 1036–1047.

[23] Mosher, R. A., Thormann, W., *Electrophoresis* 2002, *23*, 1803–1814.

[24] Bottenus, D., Jubery, T. Z., Ouyang, Y., Dong, W.-J., Dutta, P., Ivory, C. F., *Lab. Chip.* 2011, *11*, 890–898.

[25] Bottenus, D., Hossan, M. R., Ouyang, Y., Dong, W.-J., Dutta, P., Ivory, C. F., *Lab. Chip.* 2011, *11*, 3793–3801.

